Ecological Informatics 94 (2026) 103606

Contents lists available at ScienceDirect

Ecological Informatics

journal homepage: www.elsevier.com/locate/ecolinf

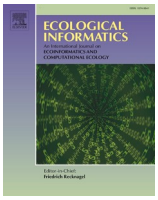

# Deep learning models used to detect fish movement over resistivity counters

Sophie A.M. Elliott [a,b,*], Keerthan Boraiah [a,b], Chun Kee Tham [a,c], William R.C. Beaumont [a,b], Paul Elsmere [d], Luke Scott [a,b], Adrian Fewings [e]

[a] Salmon & Trout Research Centre, Game and Wildlife Conservation Trust, East Stoke BH20 6BB, UK
[b] The Missing Salmon Alliance, Hampshire, UK
[c] Centre for Operational Research, Management Sciences and Information Systems, University of Southampton, University Road, SO17 1BJ, United Kingdom
[d] Environment Agency, Pennygillam Depot, Quarry Road, Launceston PL15 7ED, UK
[e] Environment Agency, Romsey Office, Canal Walk, Romsey, SO51 7LP, UK

ARTICLE INFO

*Keywords:*
Atlantic salmon
Automated detection
Convolutional neural network
Diadromous fish
Fish counters
Machine learning

ABSTRACT

Diadromous fish are one of the most threatened groups of fish species, being subject to pressures from freshwater, estuarine and marine environments. Of these fish, Atlantic salmon is the most economically important and increasingly threatened. To assess salmonid (Atlantic salmon and sea trout) stocks, resistivity counters have been widely used. However, verification of data from the counters can be challenging due to miscounts, misidentification and biases in human verification of fish counts.

We applied deep learning models to identify diadromous fish using continuous electrical resistivity data from resistivity fish counters. Our models were tested on three rivers (Frome, Fowey and Test in the South and South-West of England) and compared with a minimum of one year's manually validated data.

We detected fish signals from background noise with an F1-score of 99%, large from small fish (≥30 cm) with a precision of 95%, and an increase of >38% small and large fish waveforms. The F1-score for salmonids was 92%, and a significantly greater proportion (>173%) of upstream-moving large salmonids (≥30 cm) were detected compared to manual methods.

To date, abundance estimates for resistivity counters have only been applied to salmonids because of labour-intensive waveform identification. Using deep learning methods, we quantified salmonids and other diadromous fish with varying accuracies. Our method can be applied to resistivity counters to detect diadromous fish globally, reducing human bias and improving detection accuracy.

## 1. Introduction

Estimating the abundances of commercial fish is essential to quantifying the state of stocks and sustainable exploitation (Boulenger et al., 2024; Putt et al., 2022). Further, such abundance estimates are statutory requirements at a national and international scale (e.g., the European Marine Strategy Framework Directive (Directive 2008/56/EC) and the Common Fisheries Policy (2013/1380/EC); Probst et al., 2021). Monitoring populations can also help inform conservation and regulatory efforts to try and maintain healthy ecosystems and fish stocks (Hilborn et al., 2020; Jennings and Kaiser, 1998).

Numerous fish species have undergone a severe decline in recent years because of over-exploitation or environmental bottlenecks (Costa et al., 2021; Hilborn et al., 2020; Probst et al., 2021). Such declines have been particularly observed in diadromous fish (fish that migrate between marine and freshwater; Chalant et al., 2019). For example, Atlantic salmon (*Salmo salar*), Brown trout (*Salmo trutta*), European eel (*Anguilla anguilla*), European sturgeon (*Acipenser sturio*), river lamprey (*Lampetra fluviatilis*), sea lamprey (*Petromyzon marinus*), thin-lipped mullet (*Chelon ramada*), and shad (*Alosa* spp.; Lassalle et al., 2008; Waldman and Quinn, 2022). This group of species are often targeted for commercial exploitation as they migrate to and from their natal rivers (Gregory et al., 2023). However, the confined environment of the river phase of their migration enables easier access by commercial exploitation than that of marine species, leading to increased vulnerability from mismanagement (Putt et al., 2022). Accurate monitoring of their

* Corresponding author at: Salmon & Trout Research Centre, Game and Wildlife Conservation Trust, East Stoke BH20 6BB, UK.
*E-mail address:* sophie_elliott@yahoo.com (S.A.M. Elliott).

https://doi.org/10.1016/j.ecoinf.2026.103606
Received 4 September 2025; Received in revised form 6 January 2026; Accepted 6 January 2026
Available online 21 January 2026

populations is therefore vital to understand changes in abundance, and the effectiveness of any management measures which are put in place to protect them (Boulenger et al., 2024; Gregory et al., 2023; Putt et al., 2022).

Diadromous fish are known to migrate at certain times of year according to their latitudinal gradient temperature, discharge and other climatic factors such as the North Atlantic Oscillation (Lassalle and Rochard, 2009; Legrand et al., 2020). For example, anadromous Atlantic salmon (from here on referred to as salmon), usually migrate out in the spring as juvenile smolts, and return from their at sea migration as adults early summer and autumn, depending on whether they spend one, two or three winters at sea (Gilbey et al., 2021; Hansen and Quinn, 1998; Klemetsen et al., 2003). Migrating brown trout (known as sea trout) have a similar life cycle and migratory period as salmon, albeit they usually do not migrate to sea for as long a period, leading to smaller sizes (Aprahamian et al., 1996; Birnie-Gauvin et al., 2019; Gillson et al., 2025). European eels are catadromous semelparous fish and are known to migrate out to sea during heavy rainfall in autumn as adult silver eels, and spawn in the Sargasso Sea (Chalant et al., 2019; de Eyto et al., 2022; Righton et al., 2016). Returning juveniles migrate back to rivers across the Eastern Atlantic and Mediterranean Sea between autumn and winter, taking some 8–9 months (de Eyto et al., 2022; Righton et al., 2025). Each diadromous fish has a period during which it migrates, and adult migrants are usually monitored to assess populations (de Eyto et al., 2022; Legrand et al., 2020).

To assess the state of diadromous adult fish stock, traps, imagery data and/or counters, and rod catches are often used (Boulenger et al., 2024; Kandimalla et al., 2022; Nowak and Lankheet, 2023; Putt et al., 2022). Fish traps provide certainty in fish identification (de Eyto et al., 2022; Eatherley et al., 2005). However, they can interrupt the migration of threatened fish, are expensive, labour-intensive, and usually only operate at certain times of the year (Eatherley et al., 2005; Hellawell, 1972; Putt et al., 2022). Although rod catches are often used to assess stocks and estimate length and weight (Cefas Environment Agency, and Natural Resources Wales, 2025; ICES, 2024), they are highly dependent on correct information supplied and sufficient fish caught for accurate assessments. They also do not always consider fishing effort (Eatherley et al., 2005; Gregory et al., 2023; Thorley et al., 2005) or catchability of the fish, which may vary across the year relative to fish abundance and migration timing (Beaumont et al., 1991; Beaumont et al., 1992).

Imagery techniques are often run simultaneously with counters to verify the counts, quantify errors in counting, and ensure backup due to equipment failures or other issues (Boulenger et al., 2024; Kandimalla et al., 2022; Putt et al., 2022). Counters can be run throughout the year and do not modify migration behaviour. However, they are subject to imperfect detection, and difficulty in counting fish when they pass through too quickly, or numerous fish swim pass simultaneously (Kandimalla et al., 2022; Putt et al., 2022; Thorley et al., 2005). Although photographic verification can resolve some of these problems, turbid water conditions can impede visibility (Kandimalla et al., 2022; Li et al., 2023; Putt et al., 2022).

Numerous types of counters exist (e.g., mechanical, electrical, and sonar), the most common being resistivity counters (Beaumont et al., 1986; Eatherley et al., 2005; Kandimalla et al., 2022). They work using a series of metal electrodes (usually three) mounted on the bottom of the river, weir or hatch at 0.3–2 m depth (Beaumont, 2016; Putt et al., 2022). This creates two zones (centre electrode to upstream electrode, and centre to downstream) where the resistivity or conductivity of the water is monitored. Resistivity counters are usually placed on weirs upstream of the tidal limit, where the speed and flow of the water force the fish to ascend close to the electrodes, and the water remains relatively shallow to ensure detection (Hellawell, 1972; Eatherley et al., 2005). The electrodes use low-intensity currents, which are completely harmless to fish (Nowak and Lankheet, 2023). Each electrode is separated by a distance adapted to the minimum length of the key species to be detected (e.g., 45 cm for adult salmon). This way, as the fish pass over, a sufficiently large electrical resistance change is produced (the fish is more conductive than the water), and registered as a 'fish event' (Eatherley et al., 2005; Nowak and Lankheet, 2023; Rasmussen et al., 2012).

The shape, size, conductivity, and depth at which the fish swims over the electrode will lead to different-shaped signals being produced (Eatherley et al., 2005; Hellawell, 1972; Nowak and Lankheet, 2023). When the water passing over the fish counter is shallow enough, the length of the fish can be estimated by the size (amplitude) of the waveform signal (Aprahamian et al., 1996). However, fish swimming behaviour can change as they pass over the electrodes if there is sufficient depth. This can lead to unreliable length measurements or asymmetric waveforms as the fish travels at different depths within the water column (Aprahamian et al., 1996; Hellawell, 1972). The speed fish pass over the electrodes can also affect the signal, with faster-moving fish producing smaller signals than slower-moving fish (Beaumont et al., 1986). To date, reliable length estimations of fish on counters have not been made from waveform signals, since these need to be matched with more precise video recordings.

The electrical signal produced when an object passes over the electrodes is interpreted by an electronic device to detect and count characteristic fish signals (Beaumont et al., 1986). The counters usually ascribe a direction of travel to the counts based on the sequence in which the fish travels over the electrodes. For example, downstream, middle, upstream would be an 'upstream' count, with the opposite pattern being a 'downstream' count. To date, these waveform signals have been identified by manually visualising 1000s of these signals and pairing them with video images (Aprahamian et al., 1996; Beaumont et al., 1986; Nowak and Lankheet, 2023; Rasmussen et al., 2012). Manual interpretation can be very time-consuming in highly productive rivers, and lead to counting errors through fatigue (Kandimalla et al., 2022; Salman et al., 2016). To reduce identification error and missed counts, double counting is often used (Boulenger et al., 2024; Eatherley et al., 2005; Putt et al., 2022), but increases labour costs. Since waveform recording has been implemented, computer interpretation of electronically recorded signals and images has developed significantly. In particular, machine learning mechanisms for fish monitoring are a rapidly evolving area, particularly when using imagery (e.g. https://kb-ts.nl/; https://www.rodconnolly.com/automated-monitoring.html – Baanbrekend in camera onderzoek; Automated monitoring; Li et al., 2023; Yassir et al., 2023). Even so, to date, no prior studies have been found applying automated detection of resistivity counter waveform data.

Given the wide use of resistivity counters for salmonid stock assessments (Aprahamian et al., 1996; Cefas Environment Agency, and Natural Resources Wales, 2025; ICES, 2024), our research goal was to assess the potential of deep learning methods to identify species and groups of species from background noise, their direction of movement, and length class. Use of automated methods to analyse resistivity counters data has not previously been undertaken. Deep learning models (e.g., Random Forest, Convolutional Neural Network (CNN); XGBoost; Henriques et al., 2020; Janiesch et al., 2021; Mouy et al., 2024; Razzaq and Shah, 2025) are a type of large neural network combining several layers of simultaneous descriptors for the data and descriptors of classification (Saleh et al., 2024; Villon et al., 2018). We aimed to automate fish identification and counting through deep learning models, save time from traditional manual validation methods, and remove human bias. We tested our method on three contrasting rivers in the South and South-West of England. The River Frome and the River Test are chalk stream rivers in Dorset and Hampshire, known to have relatively stable environmental conditions and moderate conductivity (Beaumont et al., 1986; Simmons et al., 2020). The River Fowey in Cornwall is a granite-sourced river with lower conductivity than the River Frome and Test. These rivers provide key stock assessment data at a national and international level (Cefas Environment Agency, and Natural Resources Wales, 2025; ICES, 2024). Deep learning models were trialled on these

rivers since they have detailed data from which estimates of salmonid populations have been made and are available.

## 2. Methods

### 2.1. Resistivity counter study area and data

The Frome resistivity counter is located 8 km from the tidal limit on a flume gauging weir. The ambient conductivity of the River Frome ranges from 300 to 400 μScm$^{-1}$, but over the timescale of minutes is relatively stable. The Fowey resistivity counter is located on a weir 3 km from the tidal limit, with conductivity ranging from 60 to 90 μS cm$^{-1}$. The River Test resistivity counter is located approximately 2 km from the tidal limit on a gauging weir with water conductivity ranging from 400 to 550 μS cm$^{-1}$ (Fig. 1).

The raw waveform trace data for the rivers Test and Frome is extracted from a Conductance Sensor, which gives conductance measurements between the pairs of electrodes every 5.88 milliseconds (170 samples per second). The River Fowey data is recorded and downloaded from a Logie 2100c counter (Aquantic Logie Fish Counters Ltd.) and uses internal software (Aprahamian et al., 1996; Fewings, 1993) to process waveforms. Raw data from these signals is then saved in the format of .csv files and transformed to a data frame to provide formatted date, time, and the difference between the up and downstream sensor values.

To date, on the River Frome, the 'Gentle Heron' program (a serial data recording program) developed by Fewings in 2022, has been used to collect data from the sensor. An R script written by Fewings as a prototype is then used to filter the raw data into reviewable waveforms for fish counters managed by the Environment Agency. Fish waveforms are filtered from noise data by an experienced staff member who visually inspects all the waveforms using their previous knowledge. The manually processed salmonid waveforms are validated with video data by matching date and time information. Where mismatches in time occur between the video and trace data (since the timing of the equipment is not always perfectly synchronised), five seconds before and ten seconds after the trace time, and the video sequence are examined to aid in matching the data.

Three years of River Frome video and waveform data (2022–2024) were used to train the deep learning models and automate species identification (Fig. 2.a). On the River Fowey, the Gentle Heron data was only used in 2022, so only this year's data could be used for comparative purposes. For the River Test, data were only available from 1st June 2024 to 31st October 2025. All analyses were undertaken in Python v3.11 using Anaconda Navigator and Jupyter Notebook. Key Python libraries employed include 'Pandas' for data manipulation, 'NumPy' for numerical computations, 'Matplotlib' and 'Seaborn' for visualisation. Standard Python packages such as 'Os', 'Glob', 'Gzip', 'Re', and 'Datetime' were used for file handling and date-time operations (Appendix A – Supplementary data and code).

### 2.2. Detection of fish from noise and the direction of fish movement

To model noise from fish movement, a few well-known machine and deep learning models were explored to analyse which performed better at decision making and image classification predictions (Li et al., 2023; Razzaq and Shah, 2025). These models included Random Forest,

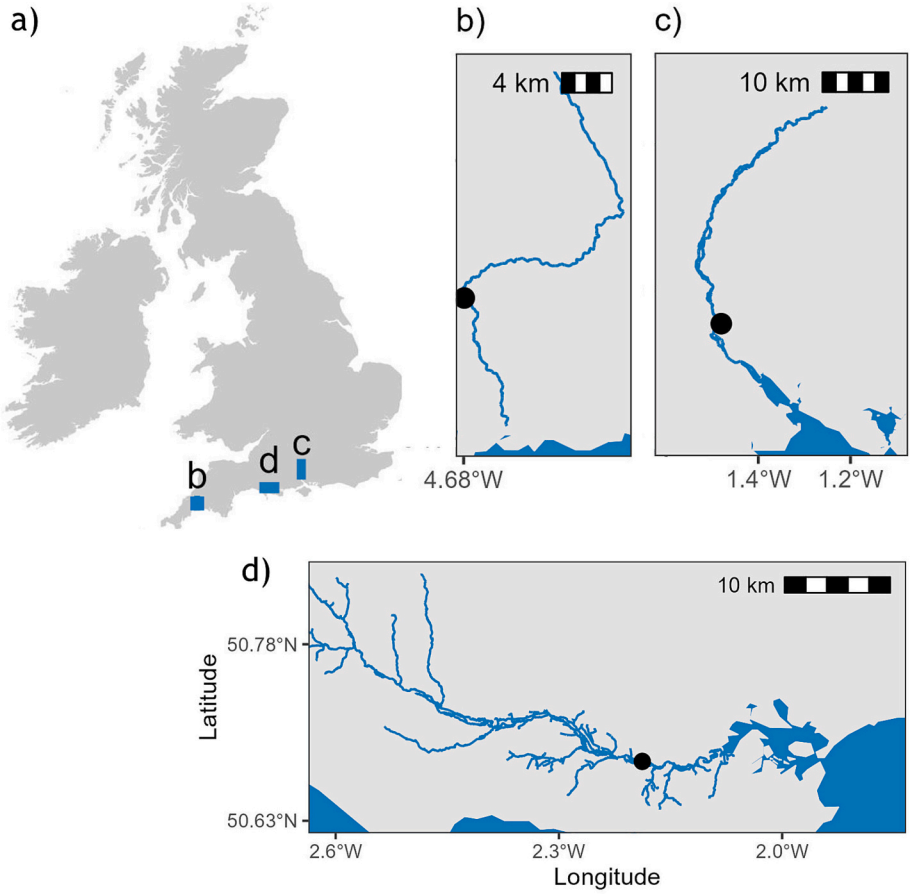


**Fig. 1.** Map showing a) the study locations of the River Frome, Fowey and Test, b) the River Fowey and resistivity counter, c) the River Test and resistivity counter, d) the River Frome and resistivity counter (black circle).

XGBoost, K-Means clustering, and one-dimensional convolutional neural networks (CNN; Ayeni, 2022; Breiman, 2001; Henriques et al., 2020; Jahanbakht et al., 2023; Mouy et al., 2024), using the packages 'Scikit-learn' and 'TensorFlow Keras' (Abadi et al., 2016; Pedregosa et al., 2011). Each of these algorithms performs differently based on its problem-solving capabilities and the data it is provided (Henriques et al., 2020; Mouy et al., 2024; Razzaq and Shah, 2025). The best performing model was pre-loaded in the 'PyTorch' deep learning framework (Paszke et al., 2019) and used throughout the process (Appendix A - Supplementary data and code).

### 2.2.1. Data preprocessing

The data were split into 10-s window periods (*US at* 10*s* and *DS at* 10*s*; DS = downstream, US = upstream) which is the maximum time a fish takes to swim over a counter (Fig. 2.b). The peak electrical activity was normalised to improve comparability and interpretability for the model across events using Eqs. 1 and 2.

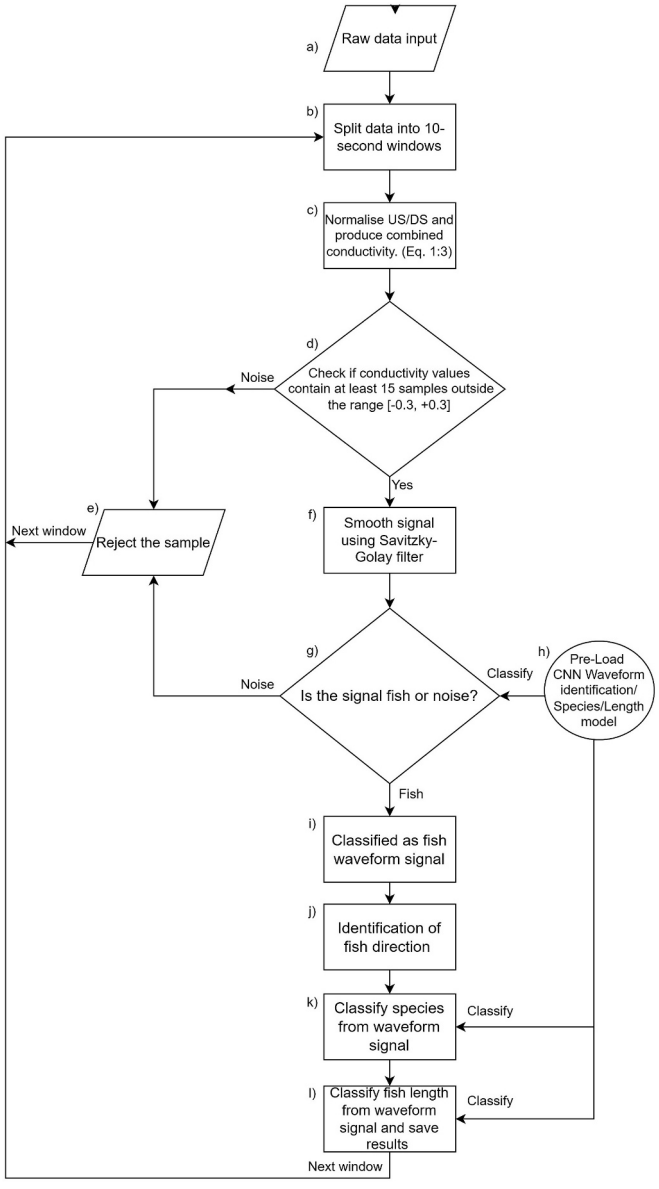


**Fig. 2.** Flow diagram to identify fish waveforms from noise waveforms and characterise them. Rectangle = process, diamond = decision, parallelogram = input/output, circle = connector, cylinder = library.

$$USP = 2^{*}((US\,at\,10s - \min USat\,10s)/(\max USat\,10s - \min US\,at\,10s)) - 1 \quad (1)$$

$$DSP = 2^{*}((DS\,at\,10s - \min DSat\,10s)/(\max DSat\,10s - \min DS\,at\,10s)) - 1 \quad (2)$$

Where *USP* = Upstream peak, *DSP*= Downstream peak, *US at* 10*s* and *DS at* 10*s* = are the downstream and upstream counts at every 10-s interval.

Eq. 3 was implemented to merge the two peaks and get the sigmoid waveform (*a*). The sigmoid waveform was divided by two to ensure that the range was between −1 to 1. To interpret the waveform, the second peak is inverted (Fig. 2.c).

$$a = \frac{((DSP + (-1^{*}USP))}{2} \quad (3)$$

An event is produced when it exceeds a normalised threshold of 0.3 units and increases consistently at successive millisecond intervals during the time it takes for a fish to swim over the electrodes. The threshold value of 0.3 units was established by reference to earlier counter devices and validated through analysis of tens of thousands of fish-like conductivity events. Electrical interference can occasionally produce noise that also surpasses the 0.3-unit threshold (Fig. 2.d). Unlike biological events, these noise-induced signals are characterised by irregular and inconsistent patterns in the conductivity profile. Therefore, when the sigmoid waveform (*a*) was less than 15 times >0.3 and < −0.3, then the signal was classified as noise (Fig. 2.e; Fig. 3.a and b). If *a* was 15 times >0.3 and < −0.3 then the signal was classified as a fish waveform (Fig. 3.c-f).

To help distinguish fish waveforms from noise clearly, the smoothing Savitzky-Golay filter was applied using the 'SciPy' package (Fig. 2.f; Virtanen et al., 2020). The filter uses a window length of 20 samples (~10th of a second), and a poly-order of two to help smooth the signal and facilitate training of the data. Smaller window lengths resulted in lower confidence in fish identification. The preloaded models were then run to classify the waveforms into noise and fish (Fig. 2.g:i).

The direction of fish movement was identified by checking for the steady rise of negative and positive peaks. If the first peak is positive, this indicates that the fish is moving upstream (*USP*) and if the first peak is negative, the fish is moving downstream (*DSP*; Fig. 2.j; Hellawell, 1972). This directional movement, however, depends on the polarity of the electrode connections.

Given the large number of labelled waveforms (over 5000), 80% of the data was used for training and 20% for testing. Stratified sampling was applied using the 'Scikit-learn' library to ensure balanced representation across classes (Pedregosa et al., 2011). The testing sample was re-split into a 50% validation sample and a 50% testing sample. All waveform sequences were standardised to a fixed length of 1700 rows, corresponding to 10-s segments, using padding techniques implemented with the 'TensorFlow' package (Abadi et al., 2016).

## 2.3. Detecting species and groups of species waveforms

Following the detection of fish-specific waveforms, they were clustered into groups of similar waveforms, which identified species or groups of species (Fig. 2.k). Since salmon and sea trout (brown trout either migrating to sea or returning) waveforms appear identical (Fig. S1) because of their similar body shape and behaviour, they were clustered into a single group (salmonids). Due to the low numbers of European eel (31 individual detections) and lamprey, which may include sea lamprey and river lamprey (20 individual detections), they were also clustered into the same group. Eels and lampreys also have similar morphologies (Kerr et al., 2015) and thus also produce similar waveforms (Fig. S1).

**Table 1**
The number of manually identified species trace waveforms, the quantity of data used to train and test the fish species class model between 2022 and 2024 on the River Frome, and the quantity of data generated to balance the species classes.

| Species | Manually trace identified fish | Training (before SMOTE) (70%) | SMOTE generated training data | Testing (30%) |
|---|---|---|---|---|
| Salmonids | 1207 | 845 | 0 | 362 |
| Mullet | 130 | 91 | 845 | 39 |
| Eels and lamprey | 52 | 36 | 845 | 16 |

To distinguish species or groups of species-specific data, a total of 1638 manually verified fish waveforms (detected through video data) were used to train the model (Table 1). As a result of the reduced dataset, training to testing data were split 70:30%, using 'train_test_split' with the stratify parameter function in 'Scikit-learn' (Pedregosa et al., 2011).

Given that deep learning models rely on large quantities of good-quality data during training (Saleh et al., 2024; Villon et al., 2018), Synthetic Minority Over-sampling Technique (SMOTE; Chawla et al., 2002; Fonseca et al., 2021) was applied to create similar replicates of waveforms for mullet, and eels and lamprey classes, since these species' classes were imbalanced (Table 1). The best deep learning models from

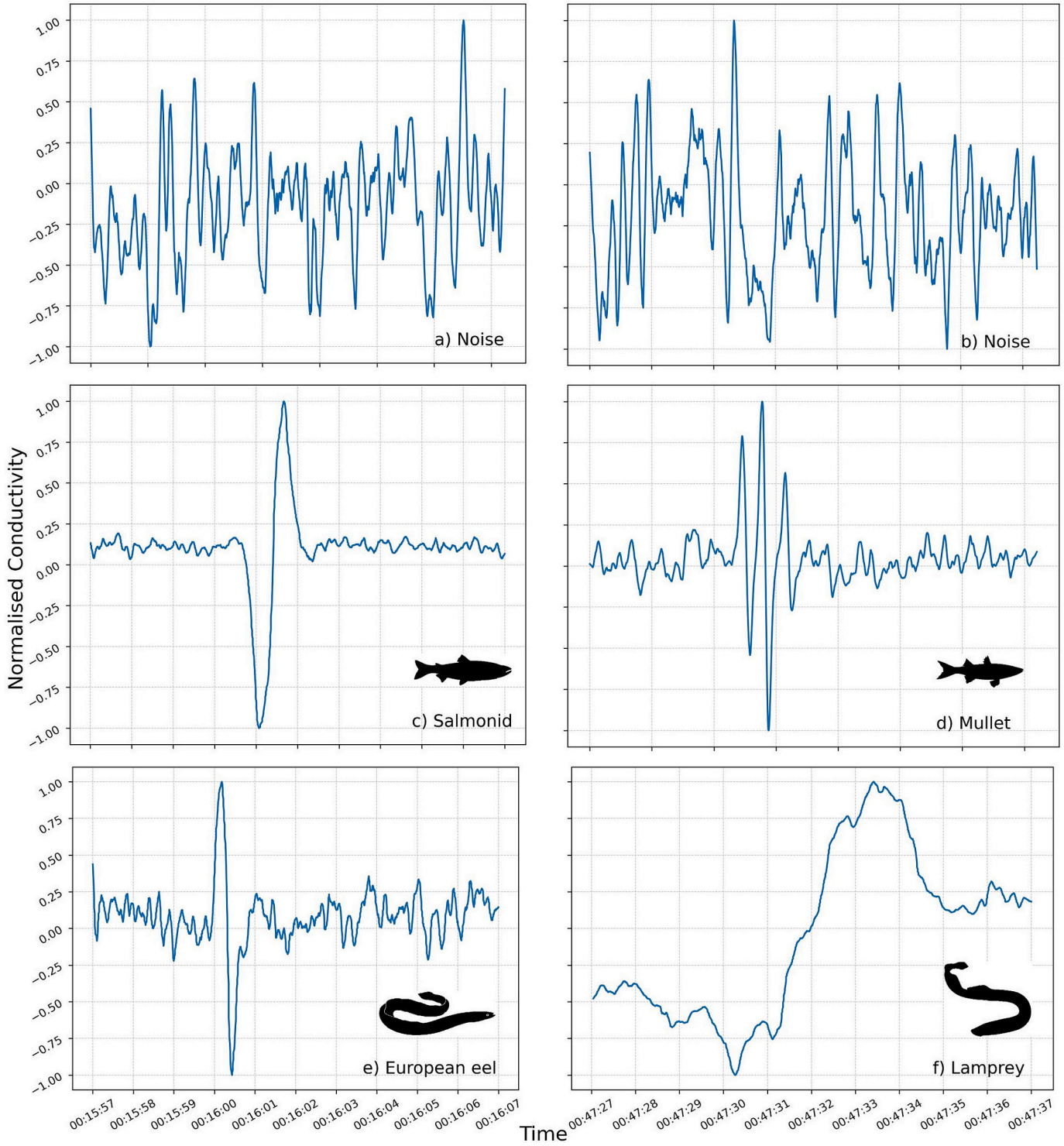


**Fig. 3.** An example of typical waveforms for noise (a and b), salmonids (c), mullet (d), European eel (e), and Lamprey (f).

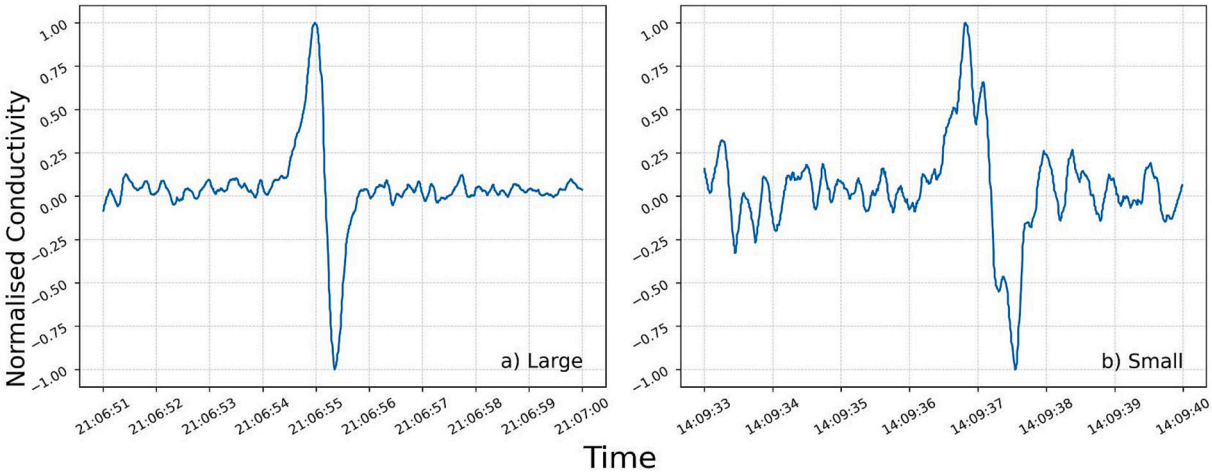


**Fig. 4.** Typical waveforms of large (≥ 30 cm; a) and small (< 30 cm; b) salmonids on the River Frome.

**Table 2**
The number of manually identified small and large fish trace waveforms, the quantity of data used to train and test fish length classes on the River Frome between 2022 and 2024, and the quantity of data generated using SMOTE to balance the length classes.

| Fish length class | Manually identified fish | Training (before SMOTE) (70%) | SMOTE generated training data | Testing (30%) |
|---|---|---|---|---|
| <30 cm | 63 | 44 | 247 | 19 |
| ≥30 cm | 353 | 247 | 0 | 106 |

the detection of fish from noise models (i.e., CNN, Random Forest and XG Boost) were then trialled for species identification. The best performing model was then used to distinguish species categories (Fig. 2.k; Appendix B – Supplementary information for deep learning architecture and hyperparameters methods).

### 2.4. Fish length classes

Since the River Frome electrode depth ranges between 0.5 and 1.5 m, precise fish lengths cannot be estimated. However, length classes of fish passing over the sensor were possible since fish <30 cm will have a lower overall conductivity than fish ≥30 cm. Waveform signals corresponding to large and small fish were extracted and labelled based on these manual measurements. These labelled signals were used to train the models to distinguish between large and small fish. Autoscaling of the waveforms was used to help distinguish the noise within the waveform. Fish ≥30 cm have higher conductance, and the noise-to-signal ratio is lower (Fig. 4.a). Fish <30 cm have a waveform alongside noise (Fig. 2.l; Fig. 4.b).

During manual interpretation, only waveforms with a large amplitude signal (e.g., 0 to −1.0, −1.0 to 1.0, and 1.0-to-0; Fig. 4.a) were inspected for video analysis, since these were deemed to be returning adult salmonids. These waveforms were then manually compared to video images to confirm the species and length category. Since the electrodes have a minimum of 38 cm distance from one another, the inter-electrode distance was used to calibrate measurements of fish length in the video data (~±5 cm accuracy due to uncertainty in the swimming height). To model the length class, existing manually measured fish were used to train the model (Fig. 2.h and l). The best-performing model to distinguish noise and fish species was used to distinguish length classes. As a result of imbalanced data (353 fish waveforms ≥30 cm, and 63 fish waveforms <30 cm), the SMOTE method was applied to create similar replicate waveforms on the training data (70%; Table 2).

### 2.5. Model evaluation

For each of the above models, the best performing model was evaluated through precision (True Positive (TP)/TP + False Negative (FN)), recall (TP / TP + True Negative (TN)) or otherwise known as sensitivity (Fielding and Bell, 1997), and specificity (True Negative (TN)/(TN + FP) or otherwise known as a true negative rate (Saleh et al., 2024). The Percentage of Correct Classification (PCC; True Positive (TP) + True Negative (TN))/(TP + TN + FP + FN), its Confidence Interval (CI; Eq. 4; Fielding and Bell, 1997; Kashani Motlagh et al., 2025), the F1 score (the

**Table 3**
Model performance to distinguish noise from fish detection on test data using Frome data from 2022 to 2024. PCC = Percentage of Correct Classification, Confidence Interval = CI. The best performing model is highlighted in bold.

| Model | Precision | Recall | Specificity | PCC | F1-Score | CI |
|---|---|---|---|---|---|---|
| Random Forest | 0.94 | 0.93 | 0.88 | 0.93 | 0.93 | [0.91, 0.95] |
| XG Boost | 0.97 | 0.97 | 0.90 | 0.94 | 0.97 | [0.92, 0.96] |
| K-Means Clustering | 0.26 | 0.50 | 0.00 | 0.51 | 0.34 | [0.47, 0.55] |
| **CNN** | **0.99** | **0.98** | **0.99** | **0.98** | **0.99** | **[0.97, 0.99]** |

**Table 4**
Model performance on test data to distinguish fish species classes using Frome data from 2022 to 2024. The best performing model is highlighted in bold.

| Model | Precision | Recall | Specificity | PCC | F1-Score | CI |
|---|---|---|---|---|---|---|
| Random Forest | 0.81 | 0.84 | 0.71 | 0.83 | 0.84 | [0.79, 0.87] |
| XG Boost | 0.79 | 0.81 | 0.77 | 0.80 | 0.81 | [0.77, 0.84] |
| **CNN** | **0.91** | **0.86** | **0.88** | **0.85** | **0.86** | **[0.82, 0.88]** |

**Table 5**
Convolutional Neural Network species-specific model accuracy using the Frome data from 2022 to 2024.

| Species group | Precision | Recall | Specificity | PCC | F1-Score | CI | Testing sample size |
|---|---|---|---|---|---|---|---|
| Salmonid | 0.96 | 0.87 | 0.78 | 0.86 | 0.92 | [0.82, 0.89] | 362 |
| Eel & Lamprey | 0.23 | 0.56 | 0.95 | 0.90 | 0.32 | [0.88, 0.93] | 16 |
| Mullet | 0.65 | 0.82 | 0.92 | 0.94 | 0.73 | [0.92, 0.96] | 39 |

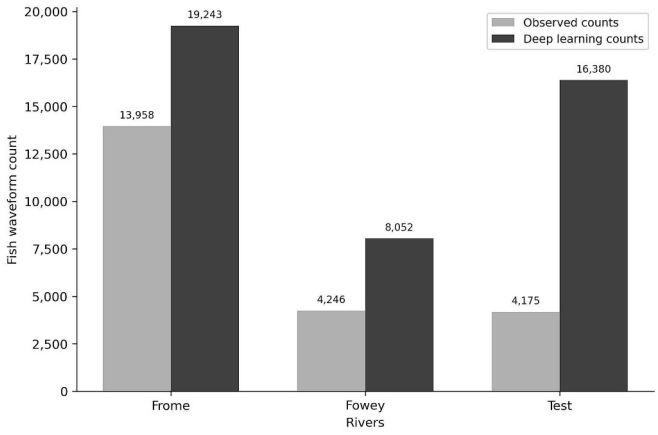


**Fig. 5.** Difference in total fish waveform counts between R-script parametric method (observed data) and deep learning modelling methods on the River Frome (38% (5285) increase in detections), Fowey (89% (3806) increase in detections), and Test (292% (16,380) increase).

harmonic mean of precision and recall; Eq. 5; Diallo et al., 2025), and confusion matrices were also used (Saleh et al., 2024; Appendix B).

$$CI = pcc \pm 1.96^{*}\frac{\sqrt{PCC^{*}(1-PCC}}{n} \tag{4}$$

$$F_1 = 2.\frac{Precision.recall}{precision + recall} = \frac{TP}{TP + \frac{1}{2}(FP + FN)} \tag{5}$$

## 3. Results

### 3.1. Detections of fish from noise

To distinguish noise data from fish signals, the CNN model performed the best in recognising the pattern in the signals compared to the other models (Table 3). The CNN model was therefore used for all three rivers, giving a total of 19,243 fish signals on the Frome between 2022 and 2024, 8052 signals on the Fowey for 2022, and 16,380 signals for the Test between 2024 and 2025 (Fig. 5; Fig. S4). Comparatively, the previously installed R-script parametric method produced 13,958 fish signals on the Frome, 4246 on the Fowey, and 4175 for the Test for the same time periods, giving a 38%, 89% and 292% increase of fish detections respectively (Fig. 5).

### 3.2. Detecting species and groups of species and their length class

CNN was also the best-performing model to identify the probability that the given waveform resembles those of the species (Table 4). Due to the high number of salmonid waveforms, the accuracy of detecting salmonids was highest when comparing against validated manual detections from video samples. Mullet had a lower accuracy due to its lower sample size, and the eel and lamprey classes had the lowest accuracy scores since they had the lowest sample size (Tables 1 and 5; Fig. S7).

The CNN model also distinguished length classes (Fig. 6) with high accuracy (Table 6; Fig. S9). Upstream returning salmonid ≥30 cm counts, significantly increased for all three rivers (the River Frome increased by 223% (2225 individuals), the Fowey by 821% (3408 individuals), and the Test by 173% (2668 individuals; Fig. 7). It should be noted that bias may have occurred during manual counts as the

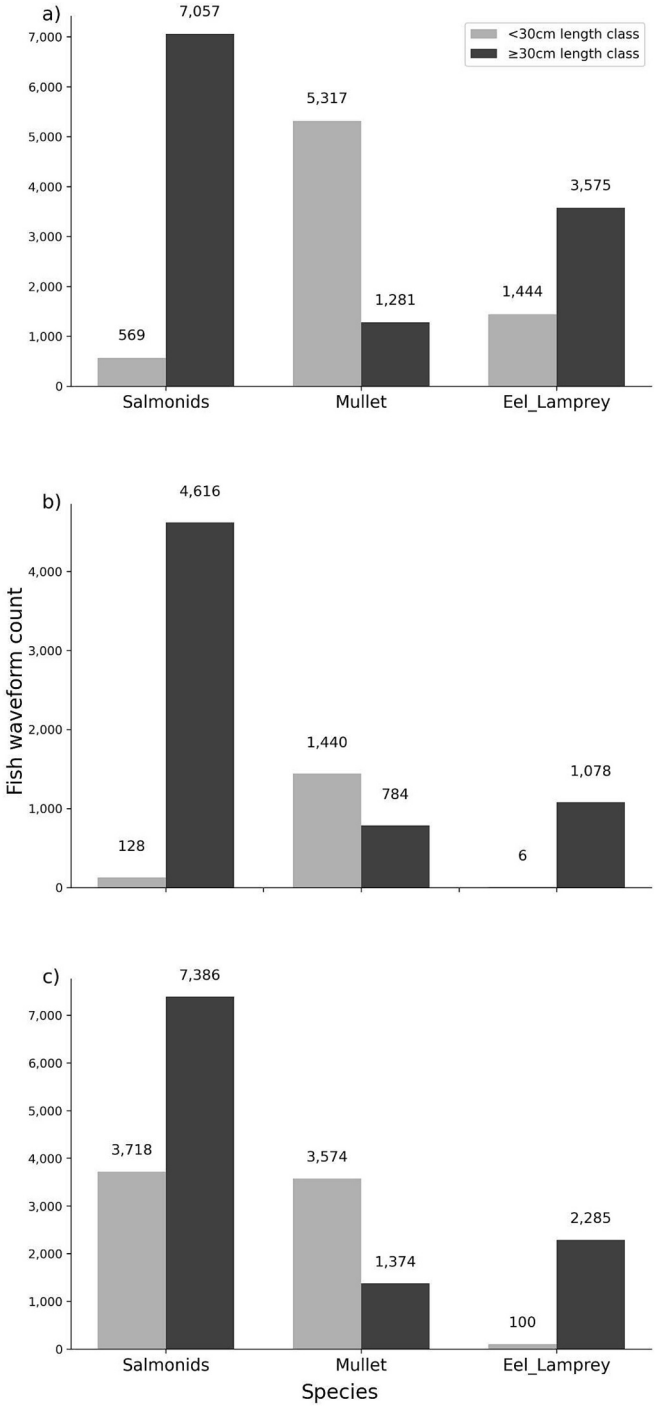


**Fig. 6.** Convolutional Neural Network species group waveform counts by length class (≥30 cm and < 30 cm) for the River (a) Frome, b) Fowey, and c) Test.

**Table 6**
Convolutional Neural Network length-specific model accuracy using the Frome data from 2022 to 2024.

| Fish length class | Precision | Recall | Specificity | PCC | F1-Score | CI | Testing sample size |
|---|---|---|---|---|---|---|---|
| Large (≥30 cm) | 0.95 | 1.00 | 0.73 | 0.96 | 0.98 | [0.92, 0.99] | 106 |
| Small (<30 cm) | 1.00 | 0.74 | 1.00 | 0.96 | 0.85 | [0.92, 0.99] | 19 |

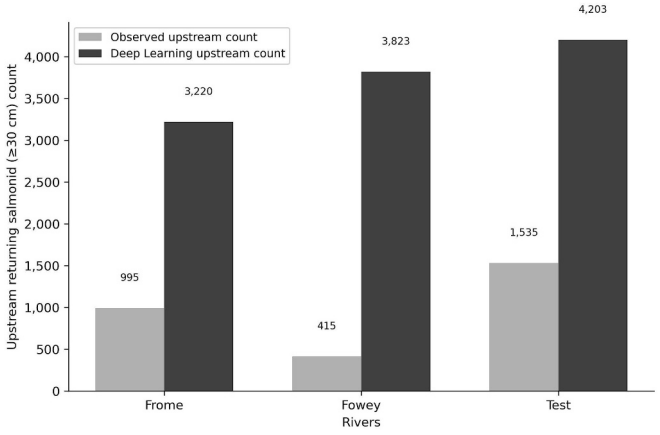


**Fig. 7.** Salmonid (≥30 cm) upstream moving trace waveform counts on the River Frome (223% (2225) increase in detections), Fowey (821% (3408) increase), and Test (173% (2668) increase), using the observed data extracted through the R-script parametric method and the deep learning modelling method.

observer may exclude detections if smaller waveforms were observed.

## 4. Discussion

Estimating population abundances is essential for the conservation and management of species (Boulenger et al., 2024; Putt et al., 2022). However, estimating these abundances can be labour-intensive, and it is often difficult to get accurate counts due to equipment malfunction and/or human error (Li et al., 2023; Villon et al., 2018). To date, automated methods interpreting waveforms from resistivity counters have not been undertaken but instead using laborious manual visual verification of waveform data (Beaumont, 2016; Eatherley et al., 2005; Nowak and Lankheet, 2023). This research aimed to develop deep learning models to automate and improve the detection of diadromous fish waveforms, reduce errors and bias to support stock estimates in a less resource-intensive manner.

Having explored a variety of different deep learning models, we found the CNN model to be the best-performing model to distinguish noise from fish waveforms and identify individual species. Furthermore, we also distinguished fish length classes, helping to determine diadromous fish life phases (e.g., salmon and trout smolt migration out to sea as juveniles (aged 1–2 years, <30 cm) and return following their ocean migration (>30 cm) with high accuracy (Gilbey et al., 2021; Hansen and Quinn, 1998; Klemetsen et al., 2003). From our analysis, we identified more salmonids than the pre-existing R-script parametric methods of counting fish for all three rivers. The CNN model was the best-performing model since it can manage unbalanced data better than the other models trialled, and it is less influenced by small changes in the input data (Kiranyaz et al., 2021; Mouy et al., 2024).

One of the key outcomes from this methodology is that it speeds up data processing, with the potential of processing real-time results, whilst removing human bias and fatigue (Kandimalla et al., 2022; Putt et al., 2022; Villon et al., 2018). For example, to process a year's worth of data, the model took less than a day to run, no matter the number of fish and fish species passing over the counter. Whereas processing this data manually could take three to six months, depending on the number of fish and the number of species required to be analysed in the river. For this reason, to date, only large salmonid waveform detections have been the focus of these most rivers. With growing concern for all diadromous fish (Costa et al., 2021; Lassalle et al., 2008; Waldman and Quinn, 2022), and the use of our proposed modelling methodology, monitoring of other species can now be undertaken.

Diadromous fish species exist across the world (Chalant et al., 2019; Lassalle and Rochard, 2009; Waldman and Quinn, 2022), and relative to other more modern methods of estimating fish abundance, such as acoustic devices, resistivity fish counters are cheaper and can function in waters with high turbidity, unlike camera techniques (Kandimalla et al., 2022; Li et al., 2023; Putt et al., 2022). Furthermore, automated trace identification methods work under a wide range of conductivities. For this method to be adapted to different rivers, calibration is required for each site to ensure correct information is supplied to the model. For example, understanding the range of depths of the water over the electrodes, and the distance between electrodes for correct length category estimations. Additionally, differences in the raw data extraction require some manipulation to extract all the relevant details.

When counters are run in parallel with videos, more precise species identification and length estimations can be made when water clarity is clear enough (Kandimalla et al., 2022; Li et al., 2023; Putt et al., 2022). At present, automated video detection on counters on the River Frome, Fowey, and Test has not been implemented, but would greatly speed up analysis and improve abundance estimations (Kandimalla et al., 2022; Li et al., 2023; Salman et al., 2016), particularly if integrated with this automated trace analysis. Some automated video analysis has been trialled using on-the-shelf packages to detect salmon in the UK (e.g., https://kb-ts.nl/ – Baanbrekend in camera onderzoek) and in other rivers globally (e.g., Soom et al., 2022). Furthermore, automated video analysis for fish detection is a well-developed area (e.g. https://www.rodconnolly.com/automated-monitoring.html; Jalal et al., 2020; Li et al., 2023; Salman et al., 2016).

### 4.1. Limitations

Although the deep learning approach to identify fish migration was very successful and characterised more waveforms than the pre-existing methods, these sorts of models require large amounts of data (1000s of waveforms) to achieve robust results (Villon et al., 2018). Species with fewer waveforms overall had lower accuracy (i.e., mullet, and eels and lamprey). Up-sampling (Chawla et al., 2002; Fonseca et al., 2021; Klasen et al., 2022) was undertaken for species with lower detections to balance the dataset (Klasen et al., 2022). Nonetheless, the performance for these species was not as good, potentially due to overfitting of the synthetic minority examples created by SMOTE. Thus, highlighting the importance of having sufficient raw waveforms for accurate modelling (Klasen et al., 2022; Li et al., 2023).

Although the CNN model identified different species or groups of species and their length categories, we could not distinguish between salmon and trout species. Their distinction was not possible because their waveforms appear identical. To distinguish salmon from trout, clear video images (ideally including a side view of the fish) are required

since these species have very similar morphologies (Klemetsen et al., 2003). Presently, salmon stock assessments for these rivers are estimated using both counter and video recordings, knowledge of when salmon migrate, and their approximate size differences (Aprahamian et al., 1996; ICES, 2024). Unfortunately, current stock assessments may overestimate salmon numbers because of misidentification with sea trout.

Another limitation of our method is that if two or more fish overlap as they move over the electrodes during the time stamp period (10th of a second), then the number of fish passing over the electrodes cannot be distinguished. This is a problem across all resistivity counters because conductivity can only be recorded every millisecond. This issue is more of a problem with mullet, which migrate in large shoals. Video verification would minimise such miscounting and support the identification of fish species.

### 4.2. Conclusion

Resistivity counters are used globally, with some 32 salmonid counters in the UK. Currently, the data from these counters is processed manually, and only considers returning adult salmonid detections rather than sea-migrating juvenile salmonids (smolt) or other diadromous fish. Our model shows how the implementation of this model could speed up data processing and yield more data in terms of species and species counts per length class. Applying this method would save on resources, revolutionise diadromous fish stock assessment practices, and improve the ecological understanding of these threatened species.

Most resistivity counters are run in parallel with video recorders to help with verification and to provide back-up if one monitoring method or another fails. Further work is required to automate imagery analysis and integrate it with these waveform deep learning models, to pave the way for new ecological applications and automated analysis for this group of threatened species.

## CRediT authorship contribution statement

**Sophie A.M. Elliott:** Writing – review & editing, Writing – original draft, Visualization, Validation, Project administration, Methodology, Investigation, Formal analysis, Conceptualization. **Keerthan Boraiah:** Writing – review & editing, Writing – original draft, Visualization, Validation, Methodology, Investigation, Formal analysis, Conceptualization. **Chun Kee Tham:** Writing – review & editing, Formal analysis. **William R.C. Beaumont:** Writing – review & editing, Data curation. **Paul Elsmere:** Writing – review & editing, Data curation. **Luke Scott:** Writing – review & editing, Data curation. **Adrian Fewings:** Writing – review & editing, Data curation.

## Declaration of competing interest

The authors declare that they have no known competing financial interests or personal relationships that could have appeared to influence the work reported in this paper.

## Acknowledgements

This project was funded by The Game and Wildlife Conservation Trust and The Missing Salmon Alliance. We would like to thank the GWCT team for their support and building a GPU to run the models in this research. We would also like to thank the Environment Agency for the extraction of and access to the River Fowey and Test data and the equipment for the collection and processing of resistivity data since 2021.

## Appendix A. Supplementary data

Supplementary material: Appendix A. Supplementary data and code. Supplementary data and code for this article can be found online: https://zenodo.org/records/17660121.

Appendix B. Supplementary material for deep learning architecture and hyperparameters methods.

## Data availability

We have shared data and the DOI for it in the supplementary materials

## References

Abadi, M., Agarwal, A., Barham, P., Brevdo, E., Chen, Z., Citro, C., Corrado, G.S., Davis, A., Dean, J., Devin, M., Ghemawat, S., 2016. Tensorflow: large-scale machine learning on heterogeneous distributed systems. arXiv. https://doi.org/10.48550/arXiv.1603.04467.

Aprahamian, M.W., Nicholson, S.M., McCubbing, D.J.F., Davidson, I., 1996. The use of resistivity fish counters in fish stock assessment. Stock Assessment in Inland Waters ed I. Cowx 27–43.

Ayeni, J., 2022. Convolutional neural network (CNN): the architecture and applications. Appl. J. Phys. Sci 4 (4), 42–50. https://doi.org/10.31248/AJPS2022.085.

Beaumont, W., 2016. Electricity Fish Research and Management, Theory and Practice, Second edition. John Wiley & Sons LTD. ISBN:9781118935583.

Beaumont, W., Mills, C., Williams, G., 1986. Use of a microcomputer as an aid to identifying objects passing through a resistivity fish counter. Aquac. Res. 17, 213–226. https://doi.org/10.1111/j.1365-2109.1986.tb00105.x.

Beaumont, W.R.C., Welton, J.S., Ladle, M., 1991. Comparison of rod catch data with known numbers of Atlantic salmon (Salmo salar) recorded by a resistivity fish counter in a southern chalk stream. In: Cowx, I.G. (Ed.), Catch Effort Sampling Strategies. Their Application in Freshwater Fisheries Management. Fishing News Books, pp. 49–60.

Beaumont, W.R.C., Welton, J.S., Ladle, M., 1992. The exploitation by rod and line of Atlantic salmon (*Salmo salar* L.) in a southern chalk stream. In: Joint Atlantic Salmon Trust/Royal Irish Academy Workshop on the Measurement and Evaluation of the Exploitation of Atlantic Salmon, Dublin, April 1991.

Birnie-Gauvin, K., Thorstad, E.B., Aarestrup, K., 2019. Overlooked aspects of the *Salmo salar* and *Salmo trutta* lifecycles. Rev. Fish Biol. Fish. 29 (4), 749–766. https://doi.org/10.1007/s11160-019-09575-x.

Boulenger, C., Roussel, J.-M., Beaulaton, L., Martignac, F., Nevoux, M., 2024. Diadromous fish run assessment: a double-observer model using acoustic cameras to correct imperfect detection and improve population abundance estimates. Front. Ecol. Evol. 11. https://doi.org/10.3389/fevo.2023.1250785.

Breiman, L., 2001. Random forests. Mach. Learn. 45, 5–32. https://doi.org/10.1023/A:1010933404324.

Cefas Environment Agency, and Natural Resources Wales, 2025. Salmon Stocks and Fisheries in England and Wales in 2024. Salmonid and Freshwater Fisheries Statistics for 2024 - GOV.UK last accessed 21/11/2025.

Chalant, A., Jézéquel, C., Keith, P., Hugueny, B., 2019. The global geography of fish diadromy modes. Glob. Ecol. Biogeogr. 28 (9), 1272–1282. https://doi.org/10.1111/geb.12931.

Chawla, N.V., Bowyer, K.W., Hall, L.O., Kegelmeyer, W.P., 2002. SMOTE: synthetic minority over-sampling technique. J. Artif. Intell. Res. 16, 321–357. https://doi.org/10.1613/jair.953.

Costa, M.J., Duarte, G., Segurado, P., Branco, P., 2021. Major threats to European freshwater fish species. Sci. Total Environ. 797, 149105. https://doi.org/10.1016/j.scitotenv.2021.149105.

de Eyto, E., Kelly, S., Rogan, G., French, A., Cooney, J., Murphy, M., Nixon, P., Hughes, P., Sweeney, D., McGinnity, P., Dillane, M., 2022. Decadal trends in the migration phenology of diadromous fishes native to the Burrishoole catchment, Ireland. Front. Ecol. Evol. 10, 915854. https://doi.org/10.3389/fevo.2022.915854.

Diallo, R., Edalo, C., Awe, O.O., 2025. Machine learning evaluation of imbalanced health data: a comparative analysis of balanced accuracy, MCC, and F1 score. In: Awe, O.O., Vance, A. (Eds.), Practical Statistical Learning and Data Science Methods. STEAM-H: Science, Technology, Engineering, Agriculture, Mathematics & Health. Springer, Cham. https://doi.org/10.1007/978-3-031-72215-8_12.

Eatherley, D.M.R., Thorley, J.L., Stephen, A.B., Simpson, I., MacLean, J.C., Youngson, A. F., 2005. Trends in Atlantic Salmon: The Role of Automatic Fish Counter Data in Their Recording. Scottish Natural Heritage Commissioned Report No. 100 (ROAME No. F01NB02).

Fewings, A., 1993. Atlantic Salmon Counting Technologies – A Contemporary Review. Atlantic Salmon Trust, Pitlochry, Perthshire. ISBN: 1 870875 22 2.

Fielding, A.H., Bell, J.F., 1997. A review of methods for the assessment of prediction errors in conservation presence / absence models. Environ. Conserv. 24, 38–49. https://doi.org/10.1017/S0376892997000088.

Fonseca, J., Douzas, G., Bacao, F., 2021. Improving imbalanced land cover classification with k-means smote: detecting and oversampling distinctive minority spectral signatures. Information 12 (7), 266. https://doi.org/10.3390/info12070266.

Gilbey, J., Utne, K.R., Wennevik, V., Beck, A.C., Kausrud, K., Hindar, K., Garcia de Leaniz, C., Cherbonnel, C., Coughlan, J., Cross, T.F., Dillane, E., 2021. The early marine distribution of Atlantic salmon in the north-East Atlantic: a genetically informed stock-specific synthesis. Fish Fish. 22 (6), 1274–1306. https://doi.org/10.1111/faf.12587.

Gillson, J.P., Blackwell, R.E., Gregory, S.D., Marsh, J.E., Bašić, T., Elliott, S.A., King, R.A., Maxwell, D.L., Riley, W.D., Stevens, J.R., Walker, A.M., 2025. Do the biological characteristics of trout (*Salmo trutta*) smolts influence their spring migration timing and maiden marine sojourn duration? J. Fish Biol. https://doi.org/10.1111/jfb.16040.

Gregory, S.D., Gillson, J.P., Whitlock, K., Barry, J., Gough, P., Hillman, R.J., Mee, D., Peirson, G., Shields, B.A., Talks, L., Toms, S., Walker, A.M., Wilson, B., Davidson, I. C., 2023. Estimation of returning Atlantic salmon stock from rod exploitation rate for principal salmon rivers in England & Wales. ICES J. Mar. Sci. 0, 1–16. https://doi.org/10.1093/icesjms/fsad161.

Hansen, L.P., Quinn, T.P., 1998. The marine phase of the Atlantic salmon (*Salmo salar*) life cycle, with comparisons to Pacific salmon. Can. J. Fish. Aquat. Sci. 55 (S1), 104–118. https://doi.org/10.1139/d98-010.

Hellawell, J.M., 1972. Automatic methods of monitoring salmon populations. In: Proceedings of the International Symposium on the Atlantic Salmon: Management, Biology and Survival of the Species, St Andrews, New Brunswick, Canada, pp. 20–22.

Henriques, J., Caldeira, F., Cruz, T., Simões, P., 2020. Combining K-means and XGBoost models for anomaly detection using log datasets. Electronics (Basel) 9, 1164. https://doi.org/10.3390/electronics9071164.

Hilborn, R., Amoroso, R.O., Anderson, C.M., Baum, J.K., Branch, T.A., Costello, C., De Moor, C.L., Faraj, A., Hively, D., Jensen, O.P., Kurota, H., Little, L.R., Mace, P., Mcclanahan, T., Melnychuk, M.C., Minto, C., Chato Osio, G., Parma, A.M., Pons, M., Segurado, S., Szuwalski, C.S., Wilson, J.R., Ye, Y., 2020. Effective fisheries management instrumental in improving fish stock status. Proc. Natl. Acad. Sci. 117, 2218–2224. https://doi.org/10.1073/pnas.1909726116/-/DCSupplemental.

ICES, 2024. Working Group on North Atlantic Salmon (WGNAS). ICES Scientific Reports, 6, p. 415. https://doi.org/10.17895/ices.pub.25730247.

Jahanbakht, M., Azghadi, M.R., Waltham, N.J., 2023. Semi-supervised and weakly-supervised deep neural networks and dataset for fish detection in turbid underwater videos. Eco. Inform. 78, 102303. https://doi.org/10.1016/j.ecoinf.2023.102303.

Jalal, A., Salaman, A., Mian, A., Shortis, M., Shafait, F., 2020. Fish detection and species classification in underwater environments using deep learning with temporal information. Eco. Inform. 57, 101088. https://doi.org/10.1016/j.ecoinf.2020.101088.

Janiesch, C., Zschech, P., Heinrich, K., 2021. Machine learning and deep learning. Electron. Mark. 31, 685–695. https://doi.org/10.1007/s12525-021-00475-2/Published.

Jennings, S., Kaiser, M.J., 1998. The effects of fishing on marine ecosystems. Adv. Mar. Biol. 201–352. https://doi.org/10.1016/S0065-2881(08)60212-6.

Kandimalla, V., Richard, M., Smith, F., Quirion, J., Torgo, L., Whidden, C., 2022. Automated detection, classification and counting of fish in fish passages with deep learning. Front. Mar. Sci. 8. https://doi.org/10.3389/fmars.2021.823173.

Kashani Motlagh, N., Davis, J., Anderson, T., Gwinnup, J., 2025. Naturally constrained reject option classification. Mach. Vis. Appl. 36 (1), 9. https://doi.org/10.1007/s00138-024-01620-5.

Kerr, J.R., Karageorgopoulos, P., Kemp, P.S., 2015. Efficacy of a side-mounted vertically oriented bristle pass for improving upstream passage of European eel (*Anguilla anguilla*) and river lamprey (*Lampetra fluviatilis*) at an experimental crump weir. Ecol. Eng. 85, 121–131. https://doi.org/10.1016/j.ecoleng.2015.09.013.

Kiranyaz, S., Avci, O., Abdeljaber, O., Ince, T., Gabbouj, M., Inman, D.J., 2021. 1D convolutional neural networks and applications: a survey. Mech. Syst. Signal Process. 151, 107398. https://doi.org/10.1016/j.ymssp.2020.107398.

Klasen, M., Ahrens, D., Eberle, J., Steinhage, V., 2022. Image-based automated species identification: can virtual data augmentation overcome problems of insufficient sampling? Syst. Biol. 71 (2), 320–333. https://doi.org/10.1093/sysbio/syab048.

Klemetsen, A., Amundsen, P.-A., Dempson, J.B., Jonsson, B., Jonsson, N., O'Connell, M. F., Mortensen, E., 2003. Atlantic salmon *Salmo salar* L., brown trout *Salmo trutta* L. and Arctic charr *Salvelinus alpinus* (L.): a review of aspects of their life histories. Ecol. Freshw. Fish 12, 1–59. https://doi.org/10.1034/j.1600-0633.2003.00010.x.

Lassalle, G., Rochard, E., 2009. Impact of twenty-first century climate change on diadromous fish spread over Europe, North Africa and the Middle East. Glob. Chang. Biol. 15 (5), 1072–1089. https://doi.org/10.1111/j.1365-2486.2008.01794.x.

Lassalle, G., Beguer, M., Beaulaton, L., Rochard, E., 2008. Diadromous fish conservation plans need to consider global warming issues: an approach using biogeographical models. Biol. Conserv. 141, 1105–1118. https://doi.org/10.1016/j.biocon.2008.02.010.

Legrand, M., Briand, C., Buisson, L., Artur, G., Azam, D., Baisez, A., Barracou, D., Bourre, N., Carry, L., Caudal, A.-L., Charrier, F., Corre, J., Croguennec, E., Der Mika'elian, S., Josset, Q., Le Gurun, L., Schaeffer, F., Laffaille, P., 2020. Contrasting trends between species and catchments in diadromous fish counts over the last 30 years in France. Knowl. Manag. Aquat. Ecosyst. 412, 7. https://doi.org/10.1051/kmae/2019046.

Li, J., Xu, W., Deng, L., Xiao, Y., Han, Z., Zheng, H., 2023. Deep learning for visual recognition and detection of aquatic animals: a review. Rev. Aquac. 15 (2), 409–433. https://doi.org/10.1111/raq.12726.

Mouy, X., Archer, S.K., Dosso, S., Dudas, S., English, P., Foord, C., Halliday, W., Juanes, F., Lancaster, D., Van Parijs, S., Haggarty, D., 2024. Automatic detection of unidentified fish sounds: a comparison of traditional machine learning with deep learning. Front. Remote Sens. 5, 1439995. https://doi.org/10.3389/frsen.2024.1439995.

Nowak, L.J., Lankheet, M., 2023. Understanding and optimizing fish counting techniques based on electrical impedance measurements. PLoS ONE 18, e0293699. https://doi.org/10.1371/journal.pone.0293699.

Paszke, A., Gross, S., Massa, F., Lerer, A., Bradbury, J., Chanan, G., Killeen, T., Lin, Z., Gimelshein, N., Antiga, L., Desmaison, A., 2019. Pytorch: an imperative style, high-performance deep learning library. Adv. Neural Inf. Proces. Syst. 32.

Pedregosa, F., Varoquaux, G., Gramfort, A., Michel, V., Thirion, B., Grisel, O., Blondel, M., Prettenhofer, P., Weiss, R., Dubourg, V., Vanderplas, J., 2011. Scikit-learn: machine learning in Python. J. Mach. Learn. Res. 12, 2825–2830.

Probst, W.N., Kempf, A., Taylor, M., Martinez, I., Miller, D., 2021. Quo Vadimus: six steps to produce stock assessments for the marine strategy framework directive compliant with descriptor 3. ICES J. Mar. Sci. 78, 1229–1240. https://doi.org/10.1093/icesjms/fsaa244.

Putt, A.E., Ramos-Espinoza, D., Braun, D.C., Korman, J., 2022. Methods for estimating abundance and associated uncertainty from passive count technologies. N. Am. J. Fish Manag. 42, 96–108. https://doi.org/10.1002/nafm.10719.

Rasmussen, J.B., Krimmer, A.N., Paul, A.J., Hontela, A., 2012. Empirical relationships between body tissue composition and bioelectrical impedance of brook trout *Salvelinus fontinalis* from a Rocky Mountain stream. J. Fish Biol. 80, 2317–2327. https://doi.org/10.1111/j.1095-8649.2012.03295.x.

Razzaq, K., Shah, M., 2025. Machine learning and deep learning paradigms: from techniques to practical applications and research Frontiers. Computers 14, 93. https://doi.org/10.3390/computers14030093.

Righton, D., Westerberg, H., Feunteun, E., Økland, F., Gargan, P., Amilhat, E., Metcalfe, J., Lobon-Cervia, J., Sjöberg, N., Simon, J., Acou, A., 2016. Empirical observations of the spawning migration of European eels: the long and dangerous road to the Sargasso Sea. Sci. Adv. 2 (10), e1501694. https://doi.org/10.1111/faf.12894.

Righton, D., Verhelst, P., Westerberg, H., 2025. The blueprint of the European eel life cycle: does life-history strategy undermine or provide Hope for population recovery? Fish Fish. https://doi.org/10.1111/faf.12894.

Saleh, A., Sheaves, M., Jerry, D., Azghadi, M.R., 2024. Applications of deep learning in fish habitat monitoring: a tutorial and survey. Expert Syst. Appl. 238, 121841. https://doi.org/10.1016/j.eswa.2023.121841.

Salman, A., Jalal, A., Shafait, F., Mian, A., Shortis, M., Seager, J., Harvey, E., 2016. Fish species classification in unconstrained underwater environments based on deep learning. Limnol. Oceanogr. Methods 14, 570–585. https://doi.org/10.1002/lom3.10113.

Simmons, O.M., Britton, J.R., Gillingham, P.K., Gregory, S.D., 2020. Influence of environmental and biological factors on the overwinter growth rate of Atlantic salmon *Salmo salar* parr in a UK chalk stream. Ecol. Freshw. Fish 29, 665–678. https://doi.org/10.1111/eff.12542.

Soom, J., Pattanaik, V., Leier, M., Tuhtan, J.A., 2022. Environmentally adaptive fish or no-fish classification for river video fish counters using high-performance desktop and embedded hardware. Eco. Inform. 72, 101817. https://doi.org/10.1016/j.ecoinf.2022.101817.

Thorley, J.L., Eatherley, D.M.R., Stephen, A.B., Simpson, I., MacLean, J.C., Youngson, A. F., 2005. Congruence between automatic fish counter data and rod catches of Atlantic salmon (Salmo salar) in Scottish rivers. ICES J. Mar. Sci. 62, 808–817. https://doi.org/10.1016/j.icesjms.2005.01.016.

Villon, S., Mouillot, D., Chaumont, M., Darling, E.S., Subsol, G., Claverie, T., Villéger, S., 2018. A deep learning method for accurate and fast identification of coral reef fishes in underwater images. Ecol. Inform. 48, 238–244. https://doi.org/10.1016/j.ecoinf.2018.09.007.

Virtanen, P., Gommers, R., Oliphant, T.E., Haberland, M., Reddy, T., Cournapeau, D., Burovski, E., Peterson, P., Weckesser, W., Bright, J., Van Der Walt, S.J., 2020. SciPy 1.0: fundamental algorithms for scientific computing in Python. Nat. Methods 17 (3), 261–272. https://doi.org/10.1038/s41592-019-0686-2.

Waldman, J.R., Quinn, T.P., 2022. North American diadromous fishes: drivers of decline and potential for recovery in the anthropocene. Sci. Adv. 8. https://doi.org/10.1126/sciadv.abl5486.

Yassir, A., Andaloussi, S.J., Ouchetto, O., Mamza, K., Serghini, M., 2023. Acoustic fish species identification using deep learning and machine learning algorithms: a systematic review. Fish. Res. 266, 106790. https://doi.org/10.1016/j.fishres.2023.106790.